Adsorption and Thermal Decomposition of 2-Chloroethyl Ethyl Sulfide on TiO_2 Surfaces

Tracy L. Thompson, Dimitar A. Panayotov, and John T. Yates, Jr.*

Surface Science Center, Department of Chemistry, University of Pittsburgh, Pittsburgh, Pennsylvania 15260

Received: March 31, 2004; In Final Form: August 4, 2004

The adsorption, desorption, and oxidative decomposition of the 2-chloroethyl ethyl sulfide molecule (2-CEES) has been investigated on the TiO_2(110) surface as well as on high area anatase and rutile powdered samples. A combination of measurement tools has been employed. It has been found that a monolayer of 2-CEES desorbs in the temperature range from 275 to 400 K with an activation energy of 105 kJ/mol. Weak repulsive interactions are measured in the monolayer. The molecule may be oxidized both by Ti−OH groups on anatase or rutile and by lattice oxygen in the TiO_2. Attack at the C−S bonds occurs as chloroethoxy and ethoxy groups are produced. At about 570 K these species further oxidize to form adsorbed COO and CO_3 species. The involvement of lattice oxygen in these reactions near 600 K has been observed by measurements of the background level in the infrared spectrum that may be used to measure the formation of trapped electron states at Ti^{3+} centers formed when adsorbate oxidation occurs by consumption of lattice oxygen. Upon heating to 900 K in vacuum, oxidation products on the TiO_2 surface are completely removed. Little difference in the reactivity patterns for anatase and rutile is found in this work.

I. Introduction

Titanium dioxide is currently utilized as a photoactive catalytic material for the destruction of organic molecules by photooxidation reactions driven by sunlight.[1−4] The thermally driven surface reactions that also occur on TiO_2 are therefore of importance in properly characterizing the full sequence of chemical events at work in the catalytic photooxidation chemistry of organic molecules. This approach has been exploited by Lin and co-workers in their recent studies on thermo- and photoreactivities of organic molecules on TiO_2.[5−7]

The 2-chloroethyl ethyl sulfide (2-CEES) molecule is a simulant for S-based mustard gas (HD) compounds and is widely used for laboratory experiments. It possesses both S-group functionality and Cl-group functionality, making its chemistry more complex than test molecules containing single reactive groups.

Only one study of 2-CEES thermal decomposition chemistry on a single crystalline surface has been published. This paper, by Zhou et al.,[8] reported significant thermal decomposition of 2-CEES on the Pt(111) surface. The work reported here is the first to investigate the thermal decomposition of the 2-CEES molecule on TiO_2(110) and powdered TiO_2 surfaces. Previous work has studied the interactions of 2-CEES with TiO_2−SiO_2 and TiO_2 powders,[9] where it was shown that 2-CEES binds to Ti−OH groups via both the chlorine and sulfur moieties in the molecule. The extent and nature of the thermal decomposition of 2-CEES were not investigated at that time.

The experiments described here combine two complementary approaches for the study of 2-CEES thermal decomposition on TiO_2. In the first, a TiO_2(110) rutile single crystal is employed, and both temperature programmed desorption mass spectrometry and Auger spectroscopy are combined to observe surface chemistry on this idealized single-crystal surface in an ultrahigh vacuum (UHV) apparatus. These experiments have the advantage of known levels of surface impurities, known crystal structure, and known surface defect density. Thermal desorption measurements for 2-CEES from TiO_2(110) have been used to derive desorption rate parameters. In the second approach, transmission infrared spectroscopy has been employed using both anatase and rutile high area TiO_2 powders. These experiments have the advantage of being able to observe characteristic bond vibration frequencies for the 2-CEES adsorbate molecule, as well as the formation of new species during 2-CEES thermal decomposition. Generally the infrared experiments on high area powders are inferior to the single-crystal experiments when desorption or reaction kinetics are to be measured because of interference by surface diffusion processes as molecules exit from the pore structure of the powder. However, because of the high surface area being investigated, small coverages of adsorbed reactant and product species may often be observed by the infrared method, leading to an understanding of the general reaction patterns of the adsorbate.

In this combined study, we find that strongly chemisorbed 2-CEES molecules decompose on TiO_2 while also thermally desorbing above about 275 K. It is found that lattice oxygen from the TiO_2 is a reactant producing oxygenated products containing R−O−C and R−C═O moieties in oxygenated compounds that eventually decompose and desorb. When Ti−OH groups are present, these oxidized species are observed to hydrogen bond to the 2-CEES molecule (through both the S moiety and the Cl moiety; see earlier work[9]), and these hydrogen-bonded Ti−OH groups then preferentially disappear as oxidation of the 2-CEES occurs in vacuum. Both the single-crystal studies and the infrared studies suggest that cleanup of the TiO_2 occurs upon heating in vacuum to 900 K.

II. Experimental Section

A. Ultrahigh Vacuum Studies on TiO_2(110). The UHV chamber used for these experiments is equipped with the following: (1) First is a shielded UTI-100C quadrupole mass spectrometer that is differentially pumped via a 60 L/s ion pump and a titanium sublimation pump (TSP). The 1.4 mm diameter aperture positioned 3 mm from the crystal center, preferentially collects products originating from the crystal surface. (2) The UHV chamber also has a cylindrical mirror analyzer for Auger electron spectroscopy (Perkin-Elmer) and (3) an ion gun for

10.1021/jp040257+ CCC: $27.50
Published on Web 10/02/2004

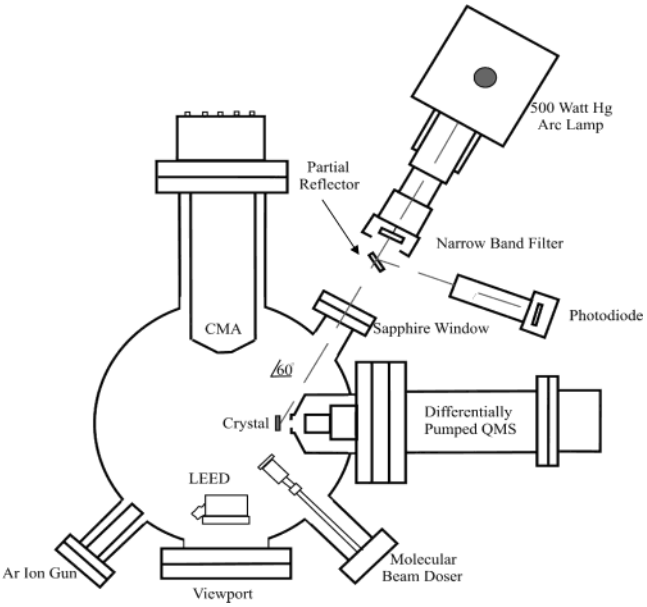

Figure 1. Schematic of ultrahigh vacuum apparatus used for studies of TiO_2(110).

sputter cleaning the crystal. The pumping system for this UHV system consists of a 360 L/s turbo pump in conjunction with a 270 L/s triode ion pump. The chamber also has an additional TSP in conjunction with a cryoshroud encircling the base of the chamber. This chamber functions at a base pressure of $<1 \times 10^{-10}$ Torr. The UHV system used for the experiments presented hereafter is shown in Figure 1. The 500 W Hg arc lamp, employed for photochemical studies, is not used in the work described here.

The single-crystal TiO_2(110) substrate ($10 \times 10 \times 1$ mm^3) used for these investigations was obtained from Princeton Scientific and cleaned under UHV conditions by repeated cycles of Ar^+ sputtering (1500 V; 3−5 μA cm^{-2}; 40 min) and annealing in vacuum to 900 K. The crystal was then oxidized by annealing to 900 K in oxygen flux (1×10^{14} molecules cm^{-2} s^{-1}) for 1 h, followed by cooling. The reduced state of the crystal was then obtained by annealing in vacuum at 900 K for 30 min. Treatment in this manner leaves the crystal free of contaminants as shown by Auger spectroscopy. The reduction state of the crystal was then tested and confirmed using a probe method developed in the laboratory that involves the thermal desorption of CO_2 which can be used to detect oxygen vacancy sites in the crystal surface.[10]

The 2-CEES compound used in both the UHV and transmission IR studies was obtained from Sigma-Aldrich (98%) and then transferred under nitrogen atmosphere into a glass bulb that was then attached to the gas line through which gas is admitted to the UHV chamber. The 2-CEES liquid was then further purified via several freeze−pump−thaw cycles. Traditionally, gases are dosed directly to the crystal surface by means of a capillary array molecular beam doser[11] which minimizes gas exposure to the rest of the chamber, in turn allowing for faster pump down times and less spurious desorption from the inside walls of the chamber. However, it was found by a systematic study that the molecular beam doser behaves in an irreproducible manner due to adsorption effects in the capillary array when 2-CEES is dosed, and as a result, a backfilling method (using a leak valve) was employed for 2-CEES gas exposure to the crystal. When calculating the overall exposure of 2-CEES to the crystal surface, both the ion gauge sensitivity and the tail of the partial pressure of 2-CEES during pump down after exposure were considered. Thermal desorption measurements were carried out using a heating rate of 3.0 K/s.

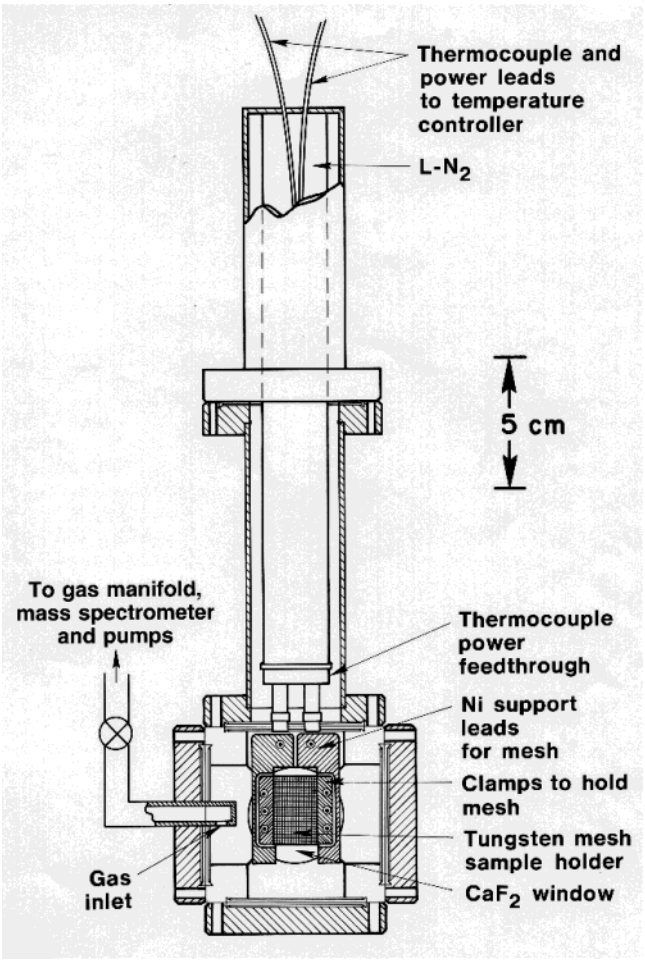

Figure 2. Schematic of high vacuum apparatus used for infrared studies of TiO_2 powders.

B. Transmission IR Studies on TiO_2 Powders. *1. IR Cell and High Vacuum System.* The transmission FTIR spectroscopic study of powder TiO_2 materials, anatase and rutile, was conducted in a stainless steel cell,[12] shown in Figure 2. The powdered TiO_2 samples are pressed into a flat tungsten grid[13] and then attached firmly to a power/thermocouple feed through via a pair of nickel leads. The temperature of the TiO_2 can be adjusted by electrical heating of the grid and by cooling with liquid N_2 or with a dry ice−acetone mixture. A programmable Honeywell digital controller operating off feedback from a K-type thermocouple welded to the top of the grid ensures temperature control with an accuracy of ±1 K. The IR cell is connected to a stainless steel high vacuum system and is capable of working under a wide range of pressures (10^{-8} to ~760 Torr). Sample temperatures from 100 to 1500 K are routinely achieved. The stainless steel vacuum system is pumped simultaneously with a Pfeiffer Vacuum 60 L/s turbomolecular pump and a Varian 20 L/s ion pump which allow a base pressure of 1×10^{-8} Torr to be achieved routinely. The base pressure was measured by the ionization current within the ion pump. Reactant gas pressure was measured by a MKS capacitance manometer (Baratron, Type 116A, range 10^{-3}−10^3 Torr).

The IR cell is aligned to the IR beam using a computer-controlled translation system (Newport Corporation) with ±1 μm accuracy[9,14] in both the horizontal and vertical positions.

Infrared spectra were obtained on a nitrogen gas purged Mattson Fourier transform infrared spectrometer (Research

Series I) equipped with a liquid N_2 cooled HgCdTe detector. The accumulation of spectra within the infrared region of 4000−500 cm^{-1} were made in the ratio mode at a resolution of 4 cm^{-1}. WinFIRST software supplied by Mattson was used for setting the spectrometer and for spectra acquisition. For each spectrum, typically 2000 scans were acquired in order to ensure precise measurement of low absorbance bands with high signal-to-noise ratio.

2. TiO_2 Powder Materials. Two different TiO_2 powder materials, anatase and rutile, were simultaneously studied by transmission FTIR spectroscopy. The anatase TiO_2 was the widely studied photoactive material Degussa P25, and the rutile TiO_2 was supplied by the Knözinger Laboratory, Institut für Materialchemie, Technical University, Vienna. The anatase TiO_2 is reported to be 99.5% pure TiO_2, having 70% anatase and 30% rutile and a surface area of ∼50 m^2 g^{-1}.[15] The average particle diameter by number count is 21 nm; 90% of the particles fall in the size range 9−38 nm. The particles exist as aggregates approximately 0.1 mm in diameter.[4] The rutile TiO_2 produced by the liquid hydrolysis of $TiCl_4$ has a surface area of 20 m^2 g^{-1} after thermal treatment in air at 823 K. According to X-ray powder diffraction, it contains only the rutile phase. The anatase and rutile TiO_2 samples are hydraulically pressed at 12 000 psi into the middle and bottom positions of the same tungsten grid as circular spots 7 mm in diameter, typically weighing 4−4.5 mg (10.4−11.7 mg/cm^2). The third, top position of the grid is empty, and it was used for reference background spectral measurements. This double-sample method involving different samples on the same grid allows close comparisons to be made for anatase and rutile under precisely the same conditions of material preparation, gas exposure, and temperature.

The oxygen used for the oxidation of annealed TiO_2 was obtained from VWSCO and was 99.8% pure.

3. TiO_2 Activation; 2-CEES Adsorption and Thermal Stability Experiments. The activation of anatase and rutile TiO_2 samples involved consecutive thermal pretreatment, oxidation, and thermal reduction procedures. The fresh samples were heated in a vacuum to the desired pretreatment temperature, 675 K, at a rate of 20 K/min and held at temperature for 4 h, and then cooled to room temperature. Oxygen at 6.2 Torr was introduced into the IR cell, and the sample temperature was increased to 675 K at a heating rate of 20 K/min. The duration of the oxidation period was 1 h; after that the samples were cooled to room temperature and O_2 was evacuated. The subsequent reduction procedure involved vacuum annealing at 822 K for 3 h, followed by cooling to room temperature. The temperature for reduction of powder TiO_2 (822 K) is slightly lower than that used for the preparation of the reduced single-crystal TiO_2(110) surface (900 K). The powdered TiO_2 samples, annealed in vacuum at 822 K, retain some Ti−OH groups which are useful in binding 2-CEES to the surface, as shown previously.[9] The reference IR spectra for oxidized and thermally reduced samples were acquired at room temperature.

The adsorption of 2-CEES on partially reduced and as well partially dehydroxylated surfaces of anatase and rutile TiO_2 samples was carried out at 255 K via several dosages of 2-CEES at increased pressures ranging from 5 to 25 mTorr. After the last dose the IR cell was evacuated to 2×10^{-8} Torr pressure. FTIR spectra were collected following each of the 2-CEES exposures as well as following evacuation.

The UHV experiments, where products were observed to desorb during temperature programming, were simulated by successive cycles of heating from 255 K to a particular temperature at 3 K/s, just as was done on the single-crystal substrate. Following this programmed heating, fast cooling to 255 K and IR spectra measurements at 255 K were then made. These experiments were carried out under dynamic vacuum conditions. Cooling to 255 K, requiring <30 s, was accomplished via a dry ice−acetone cooling mixture in the Dewar of the IR cell. In this manner, the collected information about the spectral changes for the adsorbed species on high area TiO_2 samples can be related to the information obtained by thermal programming and mass spectrometric measurements made on the TiO_2(110) crystal.

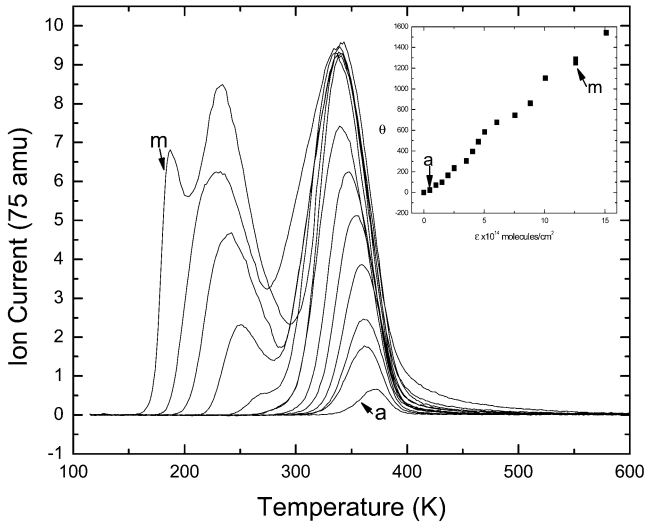

Figure 3. Thermal desorption spectra for 2-CEES adsorbed on TiO_2-(110) for exposures ranging from 0 to 1.5×10^{15} molecules/cm^2. The inset depicts the coverage versus exposure behavior for this system.

III. Results

A. TiO_2(110) Results: Adsorption, Desorption, and Thermal Decomposition of 2-CEES on Reduced TiO_2(110). The interaction between adsorbed 2-CEES and the single-crystal TiO_2(110) surface was initially studied via low-temperature adsorption (110 K) and subsequent temperature programmed desorption (TPD). For these experiments, the main cracking product of 2-CEES, mass 75, was monitored due to the low intensity of the parent ion, mass 124. Figure 3 shows the TPD spectrum of 2-CEES from a reduced TiO_2(110) surface for exposures between 0 and 1.5×10^{15} molecules/cm^2. The monolayer of 2-CEES becomes saturated at exposures of approximately 7×10^{14} molecules/cm^2 and desorbs in a single first-order kinetic process with the rate maximum at approximately 350 K. At higher exposures, a second layer develops on top of the monolayer and desorbs at approximately 230 K. Multilayer formation occurs at even higher coverages, and desorption from the multilayer occurs at approximately 170 K. Due to the approximate linearity of the coverage versus exposure plot (inset to Figure 3), we assume a unity sticking coefficient exists at the 110 K adsorption temperature. A slight discontinuity in the coverage versus exposure curve is observed as the second layer begins to form.

The thermal desorption spectra for 2-CEES from the reduced TiO_2(110) surface were simulated for low coverages (between 5×10^{13} and 3.5×10^{14} molecules/cm^2) according to the Polanyi−Wigner equation for first-order desorption:

$$R_{\mathrm{des}} = \upsilon^{\circ}\frac{1}{\beta}N \exp\left[-\frac{E_{\mathrm{des}}^{\circ} + E_{\mathrm{int}}N}{kT}\right] \qquad (1)$$

Here R_{des} is the rate of desorption (dN/dt), N is the coverage,

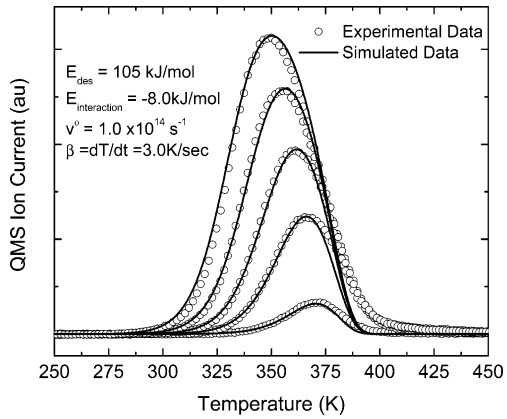

Figure 4. Simulated data versus experimental data for 2-CEES thermal desorption from TiO_2(110) for low coverages ranging from 5×10^{13} to 3.5×10^{14} molecules/cm^2.

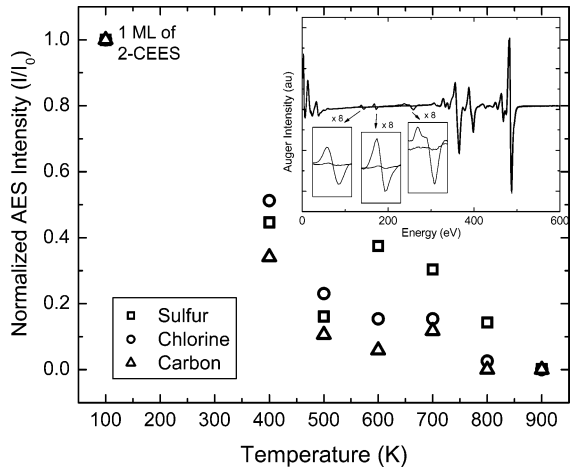

Figure 5. Change in surface coverage of S, Cl, and C as a function of annealing temperature. Points are normalized to the amount of each element measured by Auger spectroscopy for 1 ML of 2-CEES (shown at 100 K). Inset shows two representative spectra for 1 ML of 2-CEES and for the same exposure after annealing momentarily to 900 K. The enlarged regions show the same for the regions for S, Cl, and C.

ν° is the frequency factor, β is equal to dT/dt, E_{des} is the desorption energy, and E_{int} is the energy of the lateral interactions between adsorbed molecules. Figure 4 shows the results of the simulation where the zero-coverage desorption energy, E_{des}°, was found to be 105 kJ/mol, the interaction energy is repulsive and measured to be -8 kJ/mol, and the preexponential factor is on the order of 1×10^{14} s^{-1}.

For 2-CEES adsorbed on the TiO_2(110) surface, the parent molecule is completely desorbed by approximately 400 K, but at this temperature Auger electron spectroscopy (AES) shows that significant thermal decomposition products remain on the crystal, giving Auger signals for S, Cl, and C. Figure 5 displays the intensities of these 2-CEES decomposition products after heating to various temperatures. The data shown in Figure 5 are initially normalized using AES intensities measured on the layer after 1 monolayer (ML) of 2-CEES exposure to the TiO_2(110) surface without any temperature ramping. The fact that these elements are observed beyond the 2-CEES desorption range is clear evidence for the partial thermal decomposition of 2-CEES during heating. Importantly, after TPD to temperatures of 900 K, the surface becomes clean as all decomposition products are desorbed in vacuum (see insert to Figure 5). Although complete assignment to all thermal decomposition products is not possible, some insight into possible products is presented in Table 1. Thermal decomposition products presented in this table were measured by one of two methods. The presence of products was first crudely measured by analysis of the analog mass spectrum scan from mass 0 to mass 130, measured once every 5 s during temperature ramping of the crystal. Using this method, successive scans could be subtracted from one another to identify any changes, or lack thereof, for specific masses. Representative TPD spectra confirming that ethane and ethylene are produced are shown in Figure 6. Results in Table 1 provide evidence for the thermal decomposition of 2-CEES into hydrocarbon fragments, chlorinated hydrocarbon fragments, HCl, and oxygenated products. Because of the complexity of the pcoducts, we have not exhaustively studied their composition with the mass spectrometer.

B. Powdered TiO_2 Results. *1. Adsorption of 2-CEES on Partially Dehydroxylated TiO_2 Powders: Anatase and Rutile.* Adsorption of 2-CEES on high area anatase and rutile powders at 255 K produces absorption bands that are characteristic of the adsorbed molecule. In addition, hydroxyl groups are modified by the low temperature adsorption. Difference spectra clearly show the modification of the hydroxyl groups on anatase and rutile surfaces, as seen in Figure 7A. Here, the decrease in Ti−OH absorbances due to hydrogen bonding with 2-CEES are observed as several types of isolated Ti−OH groups in the 3700 cm^{-1} region are consumed, and are converted to lower frequency, spectrally broadened Ti−OH species with frequencies in the 3500−3200 cm^{-1} range. The hydrogen bonding of 2-CEES to Ti−OH groups has been reported previously.[9]

In Figure 7B, a comparison is made in the alkyl stretching region for 2-CEES in four different physical conditions. The lower spectrum shows the reference spectrum for 2-CEES gas-phase molecules, where intermolecular interactions are absent. Three alkyl modes are observed: the bands at 2978 and 2943 cm^{-1} are assigned to the asymmetric $\nu(CH_2)_{as}$ and $\nu(CH_3)_{as}$ modes respectively,[16−18] and the band at 2887 cm^{-1} is assigned to overtones of the $\delta(CH_2)_{as}$ and $\delta(CH_3)_{as}$ modes which are intensified by Fermi resonance.[16] When 2-CEES was condensed as an ice on a CaF_2 substrate, the spectrum shown in Figure 7B was obtained. A red shift of 6 cm^{-1} is observed upon condensation into the ice. Adsorption on rutile and anatase gives alkyl stretching modes that are further red shifted from the gas by 7−10 cm^{-1}. In addition, the adsorbed 2-CEES on both anatase and rutile exhibits an enhancement of intensity of the $\nu(CH_3)_{as}$ mode relative to the other two modes.

In Figure 7C the spectral developments in the fingerprint region below 1500 cm^{-1} may be compared. The bands at 1453 and 1384 cm^{-1} are assigned respectively to asymmetric and symmetric bending modes in CH_3[18,19] and the band or shoulder at 1430 cm^{-1} is assigned to the CH_2 scissor mode.[16,18] The bands near 1296 and 1269 cm^{-1} are assigned to CH_2 wagging modes,[18,19] whereas the band at about 1220 cm^{-1} is assigned to the CH_2 wagging mode of the CH_2 groups near the S atom in the molecule.[18,19] The bands in the 1070 cm^{-1} region are assigned to ν(C−C) stretching modes.[16,18] The mode assignment for 2-CEES is made in Table 2, using the gas-phase frequencies.

The hydrogen-bonded 2-CEES molecule is strongly held on the rutile and anatase surfaces. Evacuation to 2×10^{-8} Torr for 90 min at 255 K did not result in a loss of alkyl absorbance. Although the TiO_2(110) surface, discussed previously, did not have Ti−OH groups, the stability of the adsorbed layer observed on the high area TiO_2 surfaces is consistent with the beginning

TABLE 1.

compound	chemical formula	basis of identification	mass of ion fragment	additional remarks
ethane	C_2H_6	TPD: peak at 550 K	30 (29 is main fragment)	cracking pattern observed
ethylene	C_2H_4	TPD: peak at 550 K	28	cracking pattern observed
hydrogen chloride	HCl	TPD: peak at 550-600 K	36	cracking pattern observed
chloroethane	CH_3CH_2Cl	TPD: peak at 200-250 K	64	cracking pattern observed
formaldehyde (+ethane)	H_2CO (C_2H_6)	TPD: peak at 550 K	30	similar cracking pattern to ethane
acetaldehyde (+carbon dioxide)	CH_3CHO (CO_2)	TPD	44	mass 44 also CO_2, mass 29 also seen for ethane, ethylene
methane (?)	CH_4	TPD	16	may also be from cracking of other products

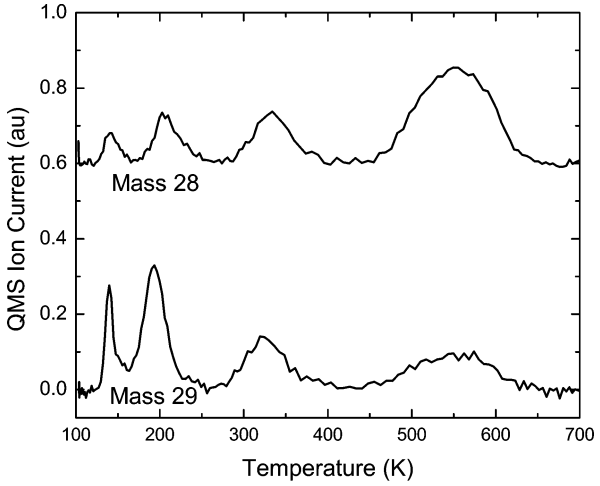

Figure 6. Representative thermal desorption spectra showing decomposition products from 2-CEES at masses 28 and 29, assigned to the thermal desorption of ethane and ethylene. Initial 2-CEES coverage = 1 ML.

of thermal desorption of 2-CEES from TiO_2(110) only at about 275 K as shown in Figures 2 and 3.

2. Thermal Activation of 2-CEES on High Area TiO_2: Anatase and Rutile. a. Anatase. Figure 8 shows the behavior of the infrared spectra as the high area anatase TiO_2 containing chemisorbed 2-CEES is heated in vacuum. All spectra were measured after cooling back to 255 K. By observing the behavior of the associated hydroxyl groups (Figure 8A), we see that at about 361 K the hydrogen-bonded Ti−OH groups begin to disappear. This loss of associated Ti−OH absorbance is not correlated with the production of isolated Ti−OH groups, since little spectral change occurs in the difference spectra shown in the 3700 cm^{-1} region. This behavior, observed from 361 to ∼514 K, suggests instead that associated Ti−OH groups are being consumed irreversibly by reaction with 2-CEES.

The irreversible behavior of the surface species (2-CEES and associated Ti−OH) may also be seen by examining the behavior of the alkyl absorbance ratios in Figure 8B. In the temperature range 255−514 K, the two lower wavenumber $\nu(CH_2)_{as}$ and overtone $(CH_3)_{as}$ and $(CH_2)_{as}$ modes increase in peak absorbance while the high-frequency mode $\nu(CH_2)_{as}$ decreases in peak absorbance. Since such changes in relative absorbance do not occur when the 2-CEES coverage increases as it is adsorbed on TiO_2 (not shown), the intensity ratio change must be due to structural and configurational changes that are not related to coverage-dependent changes in the interactions between 2-CEES molecules. We believe this intensity ratio change is related to the onset of a chemical reaction between 2-CEES and the TiO_2 surface.

Figure 8C shows similar evidence of the presence of a chemical reaction between 2-CEES and TiO_2 in the temperature range 255−514 K. It may be seen that some spectral features in the fingerprint region decrease in absorbance, while others increase. Thus, the absorbances due to the CH_2 moieties decrease in magnitude. The bands at 2966 ($\nu(CH_2)_{as}$), 1433 ($CH_{2\ scissors}$), 1299 $(CH_2)_{wag}$, and 1219 cm^{-1} $(S-CH_2)_{wag}$ all decrease together in absorbance as the temperature is increased to 514 K. Interestingly, the absorbance of the $(CH_3)_{sym}$ bending mode at 1381 cm^{-1} is almost unchanged and the same is true for the $(CH_3)_{as}$ bending mode at 1456 cm^{-1} (the small changes being due to overlap with the 1433 cm^{-1} mode which decreases in absorbance). These observations indicate that the CH_2 groups associated with both S and Cl are active in reaction with the TiO_2 surface, whereas the CH_3 group is not reactive up to about 514 K.

The increase in absorbance in the bands below 1200 cm^{-1} is related to the production of C−O moieties which exhibit stretching frequencies in this range.[5−7,16] In particular, CH_3CH_2O-Ti and $ClCH_2CH_2O-Ti$ species are indicated. The production of these ethoxy species by reaction with oxygen atoms from the TiO_2 substrate[5−7,16] is consistent with the development of enhanced absorbance due to CH_3- and $-CH_2-$ groups in the alkyl absorbance region.

Above about 514 K, a parallel progressive change in all spectral features is observed, as all spectral features of the organic species decrease together. In addition, isolated Ti−OH groups begin to be regenerated above 514 K, as may be seen in Figure 8A.

b. Rutile. As shown in Figure 9, the general behavior observed for anatase is also seen for rutile as adsorbed 2-CEES is thermally activated. Mode splitting of the C−O vibrations due to ethoxy species seems to be more evident for rutile than for anatase, and the regeneration of isolated Ti−OH groups on heating to 732 K does not seem to occur for rutile, where it is observed for anatase.

c. Spectral Development in the Carbonyl and Carboxylate/Carbonate Spectral Regions: Anatase and Rutile. As shown in Figure 10, small changes occur in the carbonyl region of the infrared spectrum as 2-CEES decomposes on both anatase and rutile TiO_2. For anatase (Figure 10A), at about 378 K, a mixture of carbonyl modes at ∼1710 and ∼1670 cm^{-1} are weakly observed. On heating to 571 K, an increase in the spectral intensity throughout the region from ∼1730 to ∼1650 cm^{-1} is observed. From 571 to 732 K, carbonyl intensity decreases. For rutile (Figure 10B), similar spectral developments are seen, with three carbonyl modes being resolved at the maximum carbonyl absorbance achieved by heating to 571−658 K. In the spectral region of carboxylate and carbonate absorbance, it is seen that the intensity of a broad infrared band increases monotonically up to 732 K for both anatase (Figure 10C) and rutile (Figure 10D). Thus we may say for both anatase and rutile TiO_2 that carbonyl-containing surface species are produced by reaction of 2-CEES with TiO_2, and that these species are then further oxidized to carboxyl/carbonate species at the highest temperatures. These observations serve to

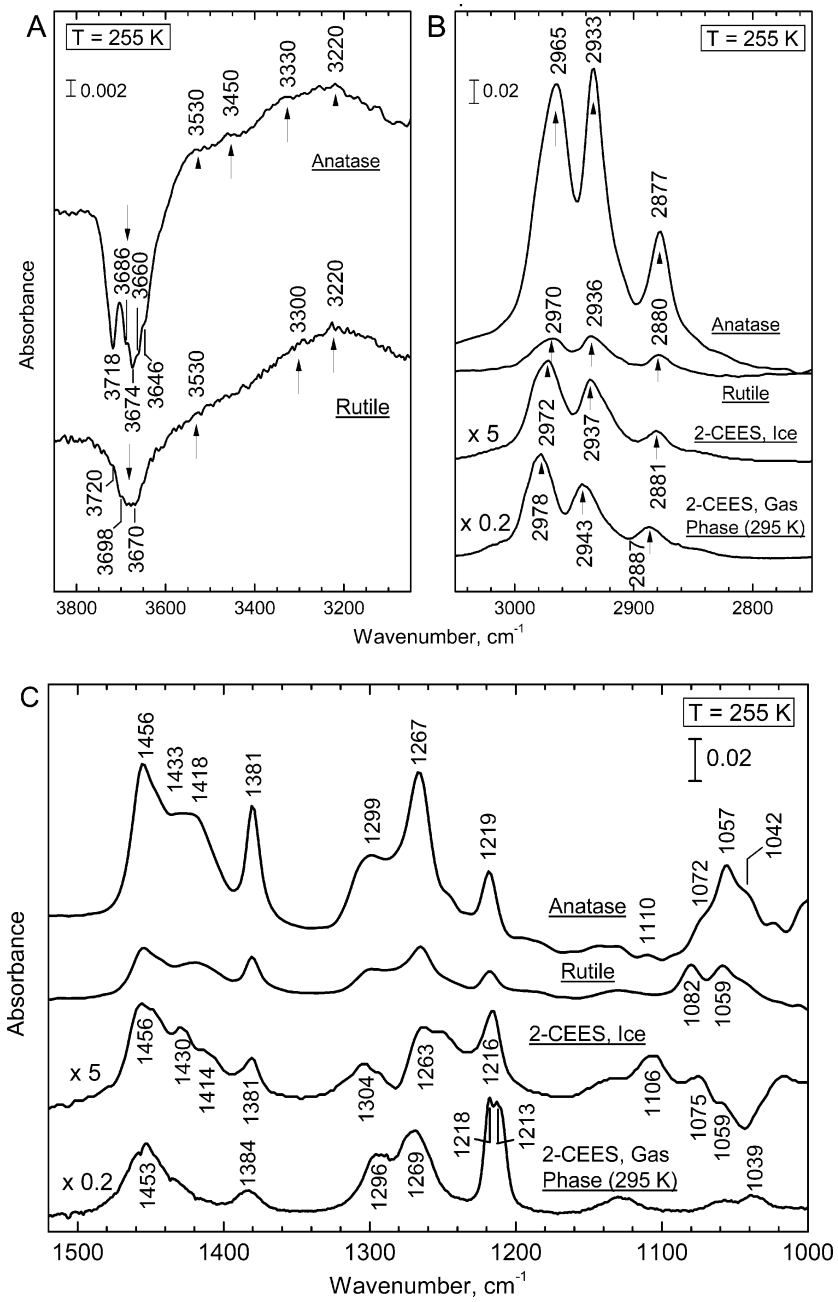

Figure 7. Difference IR spectra of 2-CEES adsorbed on TiO_2 anatase and rutile powders at 255 K.

TABLE 2: Vibration Frequencies (cm^{-1}) of 2-CEES: Gas, Ice and Species Adsorbed on TiO_2 Powders at 255 K

			adsorbed species		
mode description	gas (295 K)	ice, on CaF_2	anatase	rutile	literature[a]
$\nu(CH_2)_{as}$	2978	2972	2965	2970	2971, 2956
$\nu(CH_3)_{as}$	2943	2937	2933	2936	2917
$\nu(CH_2)_s$, overtones of $\delta(CH_2)_{as}$ and $\delta(CH_3)_{as}$	2887	2881	2877	2880	2911, 2897, 2855
$\delta(CH_3)_{as}$ bent	1453	1456	1456	1456	1484
(CH_2) scissor	1430	1430	1433	1433	1460
$\delta(CH_3)_s$ bent	1384	1381	1381	1381	1407
(CH_2) wag	1296, 1269	1304, 1263	1299, 1267	1299, 1267	1294, 1266
$S(CH_2)$ wag	1218, 1213	1216	1219	1218	1218
$\nu(C-C)_{as}$	~1040	1060	1070−1040	1080−1060	975

[a] Ab initio molecular orbital calculations from ref 18.

strengthen the argument that oxygen-containing organic species are produced when 2-CEES thermally decomposes on TiO_2, and that oxygen from Ti−OH and also lattice oxygen from TiO_2 participate in the oxidation process.

IV. Discussion

The progression of the stages of oxidation of the 2-CEES molecule can be visualized from the combination of the mass

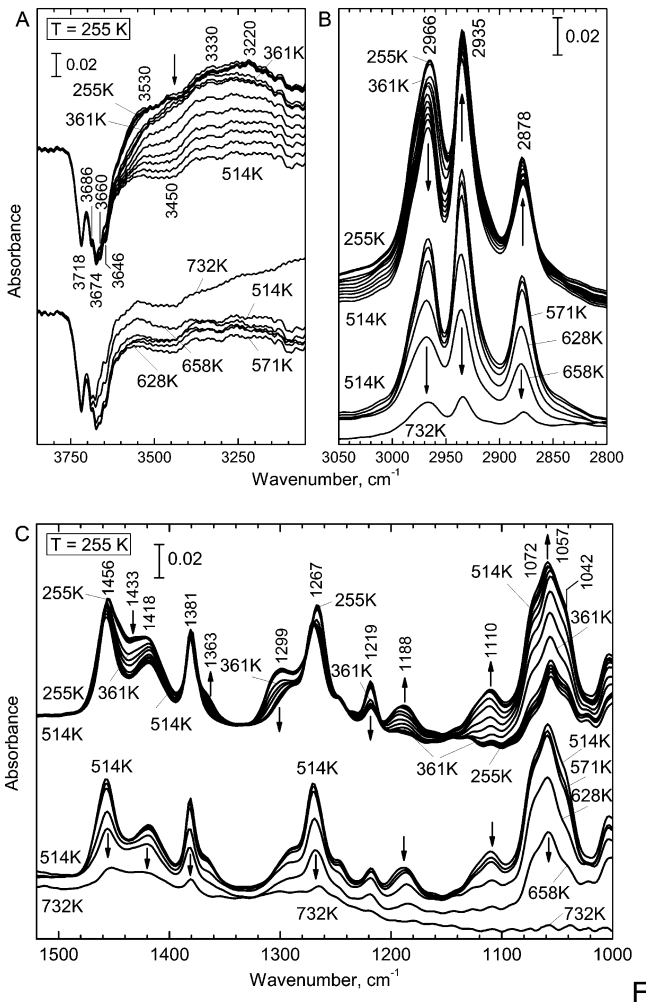

Figure 8. Difference IR spectra for 2-CEES/TiO_2 (anatase) during heating from 255 to 732 K.

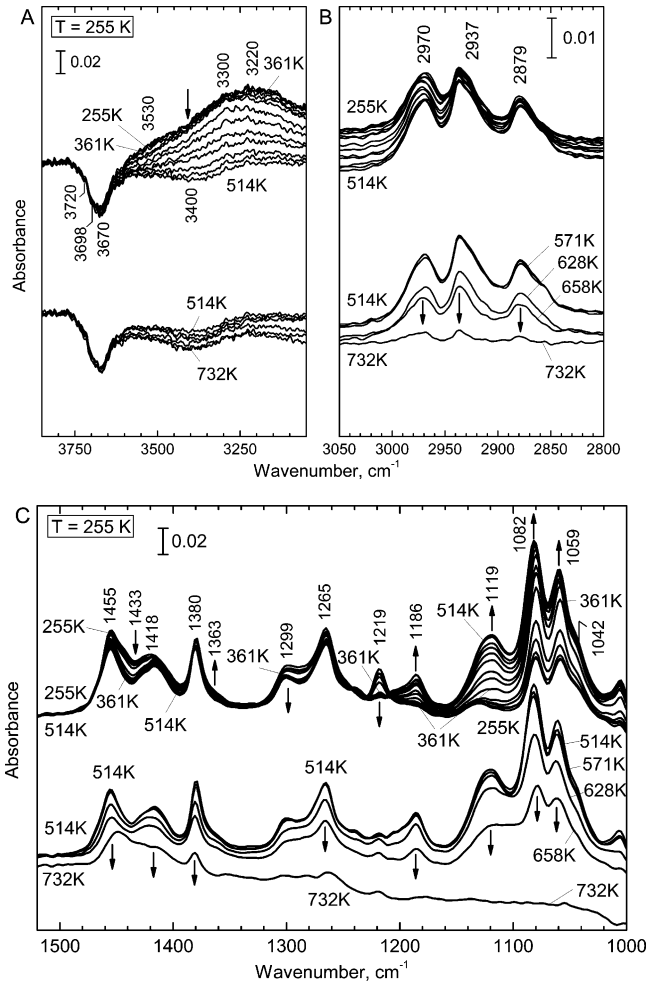

Figure 9. Difference IR spectra for 2-CEES/TiO_2 (rutile) during heating from 255 to 732 K.

spectrometric studies of the desorption of the molecule and some of its decomposition/oxidation products and the infrared studies of the species which are produced on the surface.

A. Molecular Desorption of 2-CEES. The thermal desorption studies shown in Figure 4 clearly show that 2-CEES desorption, occurring with an activation energy of ~105 kJ/mol, is complete by about 400 K from a TiO_2(110) surface which has been reduced to produce oxygen anion vacancy sites and cationic sites which may be described as Ti^{3+} sites in the surface and the bulk. Auger studies indicate (Figure 5) that species containing S, Cl, and C remain on the surface as a result of decomposition of a fairly large fraction of the monolayer of 2-CEES adsorbed. These decomposition products are removed by heating to 900 K, and the adsorptive capacity of the TiO_2 is restored for 2-CEES.

B. Reaction of 2-CEES with TiO_2. Infrared investigations, shown in Figures 7−10, performed on both anatase and rutile high area TiO_2 powders, are very revealing in showing in a general manner the functionalities that are consumed and produced when chemisorbed 2-CEES on TiO_2 is heated in vacuum.

The infrared studies utilize TiO_2 which contains isolated Ti−OH groups at fairly low coverages. In agreement with previous work, some 2-CEES molecules are hydrogen bonded to these Ti−OH groups,[9] while other 2-CEES molecules probably are chemisorbed on TiO_2 surface sites that do not possess Ti−OH groups.

At temperatures near 361 K, Ti−OH groups hydrogen bonded to 2-CEES molecules are irreversibly consumed as oxidation of 2-CEES begins to occur. It is likely that O moieties, present in the Ti−OH groups, are most reactive toward 2-CEES. In the temperature range from ~361 to ~541 K, CH_3CH_2O−Ti and $ClCH_2CH_2O$−Ti species are produced as C−S bonds in the 2-CEES molecule are broken. Near 550 K, processes involving the liberation of C_2H_6, C_2H_4, HCl, and $ClCH_2CH_3$ are observed with the mass spectrometer as these decomposition products are evolved from TiO_2(110). At the same temperature, the CH_3CH_2O−Ti and $ClCH_2CH_2O$−Ti species begin to decompose, and carbonyl and carboxylate/carbonate species begin to form. By about 732 K almost all C−O bonds and C−H bonds have been broken and infrared modes corresponding to these bonds are almost completely removed from the spectrum.

Since no oxygen from the gas phase is present in these experiments, it must be lattice oxygen in the TiO_2 that participates in the 2-CEES stepwise oxidation. On the basis of the infrared evidence, Ti−OH oxygen is most active, but OH groups cannot be involved in all of the oxidation pathways since the TiO_2(110) crystal surface, which is highly reactive in causing 2-CEES oxidative degradation, does not contain Ti−OH groups.

Wu et al.[6] have found that the surface hydroxyl groups of TiO_2 (Degussa P25) enhance the thermal decomposition of C_2H_5I molecule (previously hydrogen bonded to the OH groups) to produce surface $C_2H_5O_{(a)}$ ethoxy species at temperatures below 470 K in vacuum.

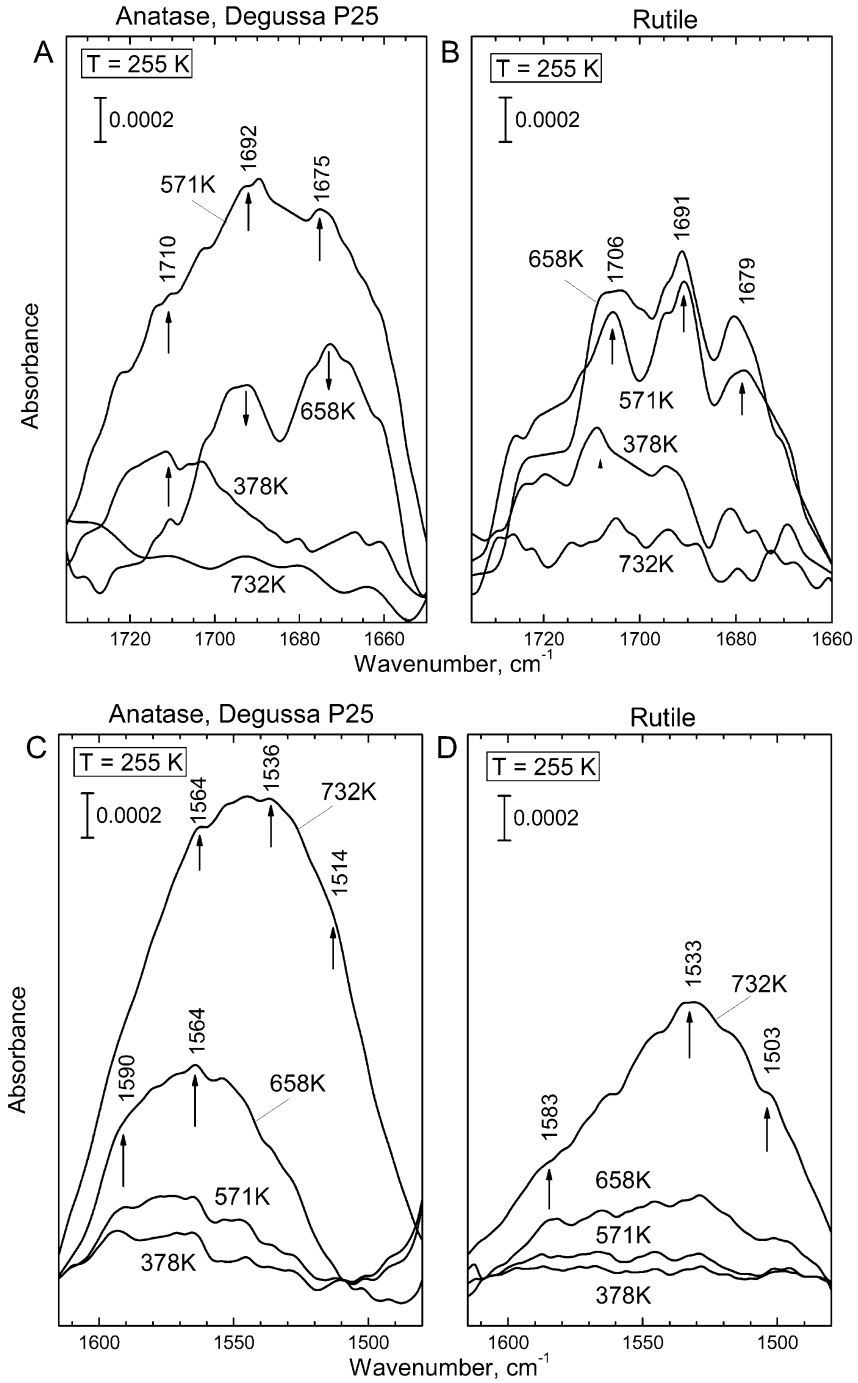

Figure 10. Difference IR spectra for carbonyl, carboxylate, and carbonate species formed during heating of 2-CEES/TiO_2 anatase and rutile powders.

Farfan-Arribas and Madix[20] have established that the defective TiO_2(110) surface is capable of strong adsorption of aliphatic alcohols at room temperature producing alkoxide and hydroxide groups. The alkoxide groups bound in a bridging oxygen vacancy ($R-O_{(b)}$) underwent reactions to produce the corresponding aldehydes, alkenes, and alcohols at temperatures above 550 K. On this basis, it is likely that ethoxy and chloroethoxy groups are also stabilized on TiO_2 when C−S bonds break in the 2-CEES molecule.

Figure 11A is a summary of the thermal processes observed by mass spectrometric observation of desorption products from TiO_2(110) containing 1 ML of 2-CEES, and from the infrared measurements on anatase and rutile high area substrates. The temperature ranges for desorption and for formation and consumption of surface intermediates are schematically shown, along with the measurement of the peak absorbance at 2966 cm^{-1} which is a general measure of the coverage of alkyl groups of all types on the surface. We find that ethoxy species formation begins below 300 K, that ethoxy species decomposition begins at about 570 K, and that COO and CO_3 formation begins at about the same temperature.

A very interesting measurement of the shift of the background in the infrared measurements is shown in Figure 11B, where the background was measured (at 2000 cm^{-1}) in the absence of interfering vibrational modes from surface species. This background intensity is caused by the formation of electron traps near the conduction band edge by the loss of lattice oxygen, and the effect has been well studied by others[21−24] as well as by ourselves.[25,26] The traps may be thought of as Ti^{3+} centers formed upon loss of lattice O. Excitation of trapped electrons

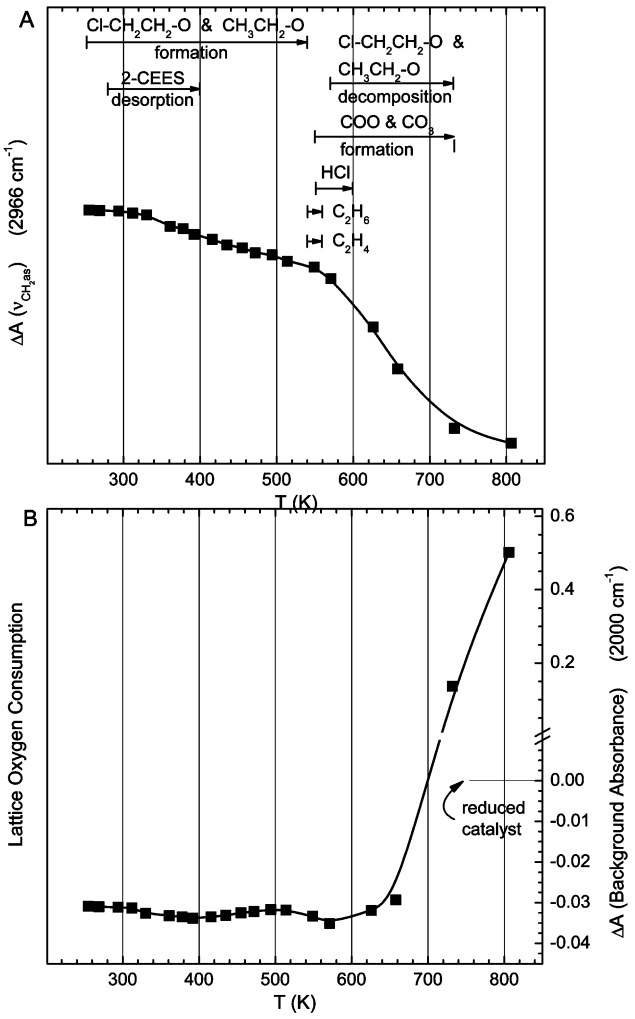

Figure 11. Schematic of thermal processes observed and formation of products upon heating of 2-CEES on TiO_2(110) and on TiO_2 anatase and rutile powders in a vacuum.

from these centers into the conduction band results in infrared absorption over a broad spectral range as infrared-induced electronic transitions occur to a continuum of conduction band electronic states. For the purposes of this paper, the changes in the absorbance of the infrared background may be used to monitor the consumption of lattice oxygen atoms by the formation of oxidized products from 2-CEES oxidation by TiO_2. Figure 11B shows that lattice oxygen begins to be consumed near ~600 K, the temperature where ethoxy species begin to be decomposed and where COO and CO_3 species begin to be formed. This is also the temperature where significant rapid consumption of surface species contributing to alkyl absorbance at 2966 cm^{-1} begins to occur by a distinct final oxidation process, as shown in Figure 11A.

These results suggest that TiO_2 should be an effective catalyst for thermal oxidation of the 2-CEES molecule under conditions where oxygen is resupplied to the catalyst from the gas phase, by the Mars−Van Krevlen oxidation mechanism.

V. Conclusions

The following results have been obtained in chemisorption studies of 2-chloroethyl ethyl sulfide on TiO_2 and the subsequent thermal oxidation using only lattice oxygen from TiO_2.

1. 2-CEES adsorbs as a monolayer that desorbs starting at ~270 K with an activation energy of 105 kJ/mol. Multilayers desorbing at lower temperatures may be adsorbed on top of the monolayer.

2. A portion of the 2-CEES monolayer is oxidized by Ti−OH groups (if present on partially dehydroxylated TiO_2). In addition, lattice oxygen from TiO_2 participates in 2-CEES oxidation at temperatures above ~570 K.

3. The 2-CEES molecule produces $ClCH_2CH_2$−O−Ti and CH_3CH_2−O−Ti (ethoxy species) by bond scission of C−S bonds.

4. Ethoxy species convert to COO and CO_3 species above ~550 K.

5. By 900 K, all oxidation products are liberated and clean TiO_2 is left in vacuum.

6. Only minor differences in the reactivity patterns of anatase and rutile TiO_2 are found in this work.

Acknowledgment. We acknowledge with thanks the support of this work by the DoD Multidisciplinary University Research Initiative (MURI) program administered by the Army Research Office under Grant DAAD 19-01-0-0619. We also thank Professor E. Knözinger and Dr. Oliver Diwald from the Technical University of Vienna for supplying the rutile TiO_2 powder for characterization.

References and Notes

(1) Fox, M. A.; Dulay, M. T. *Chem. Rev.* **1993**, *93*, 341−357.
(2) Hoffmann, M. R.; Martin, S. T.; Choi, W.; Bahnemann, D. W. *Chem. Rev.* **1995**, *95*, 69−96.
(3) Linsebigler, A.; Lu, G.; Yates, J. T., Jr. *Chem. Rev.* **1995**, *95*, 735−758.
(4) Mills, A.; Le Hunte, S. *J. Photochem. Photobiol. A: Chem.* **1997**, *108*, 1−35.
(5) Wu, W.-C.; Chuang, C.-C.; Lin, J.-L. *J. Phys. Chem. B* **2000**, *104*, 8719−8724.
(6) Wu, W.-C.; Liao, L.-F.; Lien, C.-F.; Lin, J.-L. *Phys. Chem. Chem. Phys.* **2001**, *3*, 4456−4461.
(7) Chen, M.-T.; Lien, C.-F.; Liao, L.-F.; Lin, J.-L. *J. Phys. Chem. B* **2003**, *107*, 3837−3843.
(8) Zhou, X.-L.; Sun, Z.-J.; White, J. M. *J. Vac. Sci. Technol., A* **1993**, *11*, 2110−2116.
(9) Panayotov, D. A.; Yates, J. T., Jr. *J. Phys. Chem. B* **2003**, *107*, 10560−10564.
(10) Thompson, T. L.; Diwald, O.; Yates, J. T., Jr. *J. Phys. Chem. B* **2003**, *107*, 11700−11704.
(11) Yates, J. T., Jr. *Experimental Innovations in Surface Science*; AIP Press: New York, 1998; pp 603−608.
(12) Mawhinney, D. B.; Rossin, J. A.; Gerhart, K.; Yates, J. T., Jr. *Langmuir* **1999**, *15*, 4617−4621.
(13) Ballinger, T. H.; Wong, J. C. S.; Yates, J. T., Jr. *Langmuir* **1992**, *8*, 1676−1678.
(14) *Newport Corporation Motion Control 1997 Catalog*; Section 5, page 8.
(15) *Highly Dispersed Metallic Oxides Produced by Aerosil Process*; Degussa Technical Bulletin Pigments No. 56; Degussa: 1990; p 13.
(16) Wu, W.-C.; Liao, L.-F.; Shiu, J.-S.; Lin, J.-L. *Phys. Chem. Chem. Phys.* **2000**, *2*, 4441−4446.
(17) Wong, J. C. S.; Linsebigler, A.; Lu, G.; Fan, J.; Yates, J. T., Jr. *J. Phys. Chem.* **1995**, *99*, 335−344.
(18) Sosa, C.; Bartlett, R. J.; KuBulat, K.-H.; Person, W. B. *J. Phys. Chem.* **1989**, *93*, 577−588.
(19) Kozlov, D. V.; Vorontsov, A. V.; Smirniotis, P. G.; Savinov, E. V. *Appl. Catal. B: Environ.* **2003**, *22*, 77−87.
(20) Farfan-Arribas, E.; Madix, R. J. *J. Phys. Chem. B* **2002**, *106*, 10680−10692.
(21) Szczepankiewicz, S. H.; Colussi, A. J.; Hoffmann, M. R. *J. Phys. Chem. B* **2000**, *104*, 9842−9850.
(22) Szczepankiewicz, S. H.; Moss, J. A.; Hoffmann, M. R. *J. Phys. Chem. B* **2002**, *106*, 2922−2927.
(23) Yamakata, A.; Ishibashi, T.-A.; Onishi, H. *J. Phys. Chem. B* **2001**, *105*, 7258−7262.
(24) Ghiotti, G.; Chiorino, A.; Boccuzzi, F. *Surf. Sci.* **1993**, *287/288*, 228−234.
(25) Panayotov, D. A.; Yates, J. T., Jr. *Chem. Phys. Lett.* **2003**, *381*, 154−162.
(26) Panayotov, D. A.; Yates, J. T., Jr. *J. Phys. Chem. B* **2003**, *108*, 2998−3004.